Atmos. Chem. Phys., 17, 2297–2310, 2017
www.atmos-chem-phys.net/17/2297/2017/
doi:10.5194/acp-17-2297-2017

Atmospheric Chemistry and Physics Open Access EGU

Constraining uncertainties in particle-wall deposition correction during SOA formation in chamber experiments

Theodora Nah[1], Renee C. McVay[2], Jeffrey R. Pierce[3], John H. Seinfeld[2,4], and Nga L. Ng[1,5]

[1]School of Chemical and Biomolecular Engineering, Georgia Institute of Technology, Atlanta, GA, USA
[2]Division of Chemistry and Chemical Engineering, California Institute of Technology, Pasadena, CA, USA
[3]Department of Atmospheric Science, Colorado State University, Fort Collins, CO, USA
[4]Division of Engineering and Applied Science, California Institute of Technology, Pasadena, CA, USA
[5]School of Earth and Atmospheric Sciences, Georgia Institute of Technology, Atlanta, GA, USA

Correspondence to: Nga L. Ng (ng@chbe.gatech.edu)

Received: 14 September 2016 – Discussion started: 19 September 2016
Revised: 6 January 2017 – Accepted: 16 January 2017 – Published: 14 February 2017

Abstract. The effect of vapor-wall deposition on secondary organic aerosol (SOA) formation has gained significant attention; however, uncertainties in experimentally derived SOA mass yields due to uncertainties in particle-wall deposition remain. Different approaches have been used to correct for particle-wall deposition in SOA formation studies, each having its own set of assumptions in determining the particle-wall loss rate. In volatile and intermediate-volatility organic compound (VOC and IVOC) systems in which SOA formation is governed by kinetically limited growth, the effect of vapor-wall deposition on SOA mass yields can be constrained by using high surface area concentrations of seed aerosol to promote the condensation of SOA-forming vapors onto seed aerosol instead of the chamber walls. However, under such high seed aerosol levels, the presence of significant coagulation may complicate the particle-wall deposition correction. Here, we present a model framework that accounts for coagulation in chamber studies in which high seed aerosol surface area concentrations are used. For the α-pinene ozonolysis system, we find that after accounting for coagulation, SOA mass yields remain approximately constant when high seed aerosol surface area concentrations ($\geq 8000\,\mu m^2\,cm^{-3}$) are used, consistent with our prior study (Nah et al., 2016) showing that α-pinene ozonolysis SOA formation is governed by quasi-equilibrium growth. In addition, we systematically assess the uncertainties in the calculated SOA mass concentrations and yields between four different particle-wall loss correction methods over the series of α-pinene ozonolysis experiments. At low seed aerosol surface area concentrations ($< 3000\,\mu m^2\,cm^{-3}$), the SOA mass yields at peak SOA growth obtained from the particle-wall loss correction methods agree within 14 %. However, at high seed aerosol surface area concentrations ($\geq 8000\,\mu m^2\,cm^{-3}$), the SOA mass yields at peak SOA growth obtained from different particle-wall loss correction methods can differ by as much as 58 %. These differences arise from assumptions made in the particle-wall loss correction regarding the first-order particle-wall loss rate. This study highlights the importance of accounting for particle-wall deposition accurately during SOA formation chamber experiments and assessing the uncertainties associated with the application of the particle-wall deposition correction method when comparing and using SOA mass yields measured in different studies.

1 Introduction

Secondary organic aerosol (SOA), which constitutes a large mass fraction of fine atmospheric particulate matter, is formed from the oxidation of volatile and intermediate-volatility organic compounds (VOCs and IVOCs) followed by gas-particle partitioning (Kanakidou et al., 2005; Kroll and Seinfeld, 2008; Hallquist et al., 2009; Tsigaridis et al., 2014). Laboratory chambers are typically used to study SOA formation from VOC and IVOC oxidation in a controlled environment. SOA mass yields (Y), defined as the ratio of mass concentration of SOA formed (ΔM_o) to the mass concentration of reacted hydrocarbon (ΔHC) ($Y = \Delta M_o/\Delta$HC), are

measured in these chamber experiments (Odum et al., 1996, 1997a, b). Interpretation of data derived from such experiments is complicated by the fact that particles and SOA-forming vapors deposit on the chamber walls throughout an experiment (Crump and Seinfeld, 1981; McMurry and Grosjean, 1985; McMurry and Rader, 1985; Cocker et al., 2001; Weitkamp et al., 2007; Pierce et al., 2008; Hildebrandt et al., 2009; Loza et al., 2010, 2012; Matsunaga and Ziemann, 2010; Kokkola et al., 2014; McVay et al., 2014, 2016; Yeh and Ziemann, 2014, 2015; Zhang et al., 2014, 2015; Krechmer et al., 2016; La et al., 2016; Ye et al., 2016; Nah et al., 2016). Failure to account for particle- and vapor-wall losses accurately will result in incorrect SOA mass yields, which will lead to flawed predictions of ambient SOA mass concentrations (Cappa et al., 2016).

Particles deposit on the chamber walls via diffusion, gravitational settling and electrostatic forces (Crump and Seinfeld, 1981; McMurry and Grosjean, 1985; McMurry and Rader, 1985; Pierce et al., 2008). The rate at which particles deposit on chamber walls depends on particle size. The particle-wall loss mechanism for uncharged particles in an uncharged chamber is similar to that of the dry deposition of particles (Pierce et al., 2008; Seinfeld and Pandis, 2016). Small particles are transported by Brownian diffusion through the boundary layer adjacent to the chamber walls, while the loss of large particles is governed by gravitational settling. Particle-wall loss rates are enhanced if the particles and/or chamber walls are charged (McMurry and Grosjean, 1985; McMurry and Rader, 1985; Pierce et al., 2008). Smaller charged particles deposit more efficiently than larger charged particles due to their larger Brownian diffusion rates and charge-to-mass ratios.

Several methods have been used to account for particle-wall deposition in SOA formation studies. In one particle-wall loss correction method, the rate of decay of polydisperse inert seed aerosol (e.g., ammonium sulfate particles) is measured in periodic seed-only experiments (Keywood et al., 2004; Pierce et al., 2008). Size-dependent particle-wall deposition coefficients are then obtained by fitting a first-order exponential decay to the measured particle number concentration decay in each size bin. The total aerosol number concentration usually needs to be sufficiently low in these seed-only experiments such that the effect of coagulation is negligible. In cases in which high seed aerosol number concentrations are used, an aerosol dynamics model can be applied to correct the particle-wall deposition coefficients for coagulation. Particle-wall loss in a SOA formation experiment is then accounted for using these size-dependent particle-wall deposition coefficients to obtain the total SOA mass concentration. A key assumption of this approach is that the size-dependent particle-wall deposition coefficients do not change between these seed-only and SOA formation experiments. Other previously reported particle-wall loss correction methods do not require the use of separate seed-only experiments to characterize particle-wall loss rates. Instead, the average loss rate of the total aerosol mass or number concentration is measured directly during the SOA formation experiment (Carter et al., 2005; Pathak et al., 2007; Pierce et al., 2008; Hildebrandt et al., 2009). The measured average particle loss rate is then applied to the entire experiment to correct for particle-wall deposition. A key assumption of this approach is that the particle-wall loss rate is not strongly dependent on particle size, thus allowing for the overall particle-wall loss to be characterized by a single decay rate coefficient. The extent to which these methods account for particle-wall deposition in SOA formation studies performed in a chamber, in which particle-wall loss rates are known to strongly depend on particle size, is unclear. Therefore, SOA mass yield uncertainties associated with the application of different particle-wall loss correction methods need to be evaluated when comparing and using SOA mass yields measured in different studies. This is the subject of the present work.

Previous studies have shown that SOA mass yields can be substantially underestimated if the loss of SOA-forming vapors to chamber walls is not accounted for (Matsunaga and Ziemann, 2010; McVay et al., 2014, 2016; Yeh and Ziemann, 2014, 2015; Zhang et al., 2014, 2015; Krechmer et al., 2016; La et al., 2016; Ye et al., 2016; Nah et al., 2016). Unlike particle-wall loss, experimental methods for estimating vapor-wall loss rates in chambers are not yet well established. However, the extent to which vapor-wall loss impacts SOA mass yields can be characterized and quantified using time-dependent parameterizable models that use the measured SOA mass concentrations as model inputs (Zhang et al., 2014). Recent studies have shown that the addition of large concentrations of seed aerosol can promote gas-particle partitioning and consequently increase SOA mass yields in VOC systems where the condensation of SOA-forming vapors onto seed aerosol is kinetically limited (i.e., the timescale for gas-particle equilibrium is competitive with or greater than those for reaction and vapor-wall loss) (Riipinen et al., 2011; Zhang et al., 2012, 2014; McVay et al., 2014). In contrast, SOA growth is independent of seed aerosol surface area in VOC systems in which the condensation of SOA-forming vapors onto seed aerosol is governed by quasi-equilibrium growth (i.e., the timescale for gas-particle equilibrium is less than those for reaction and vapor-wall loss) (Riipinen et al., 2011; Zhang et al., 2012; McVay et al., 2014, 2016; Nah et al., 2016). Together, these studies show that the role of gas-particle partitioning (i.e., kinetically limited vs. quasi-equilibrium SOA growth) in influencing vapor-wall deposition can be inferred from the relationship between SOA mass yields and seed aerosol surface area. However, the use of high seed aerosol surface area concentrations in chamber studies may complicate the particle-wall loss correction since (depending on the particle-wall loss correction method used) the role of coagulation may need to be accounted for. It also needs to be established how particle-wall deposition rates may change when different seed aerosol concentrations (i.e., number, surface area and volume concentrations) and

size distributions are used. These uncertainties underscore the need to better constrain the uncertainties associated with particle-wall loss correction since this correction will affect the evaluation of the magnitude by which vapor-wall loss impacts chamber-derived SOA mass yields.

In this work, we present results from targeted chamber experiments, demonstrating the change in size-dependent particle-wall deposition rates with different seed aerosol concentrations (i.e., number, surface area and volume concentrations) and size distributions. We also demonstrate how coagulation can be (and needs to be) accounted for in experiments in which high seed aerosol surface area concentrations are used to promote the condensation of SOA-forming vapors onto seed aerosol. Finally, we compare SOA mass concentrations and yields in the canonical α-pinene ozonolysis system obtained using four different particle-wall deposition correction methods and examine the uncertainties associated with each method. This work builds on our previous study on the influence of seed aerosol surface area concentration and hydrocarbon oxidation rate on vapor-wall deposition and SOA mass yields in the α-pinene ozonolysis system (Nah et al., 2016). In our previous study, we used a coupled vapor–particle dynamics model to show that the condensation of SOA-forming vapors onto seed aerosol in the α-pinene ozonolysis system is dominated by quasi-equilibrium growth. This present work is aimed at understanding the uncertainties in the SOA mass yields due to the application of different particle-wall deposition correction methods.

2 Experimental

Experiments were carried out in the Georgia Tech Environmental Chamber (GTEC) facility (Boyd et al., 2015). A single FEP Teflon chamber (volume 13 m^3) was used for the entire study. Prior to each experiment, the chamber was flushed with dried, purified air for >24 h until the aerosol number concentration was $<30\,cm^{-3}$. Experiments were performed at <5 % RH and 25 °C. NO_x mixing ratios in these experiments were <1 ppb.

The dark α-pinene ozonolysis experimental procedure used in this study was similar to that used in Nah et al. (2016). First, 22 ppm of cyclohexane (Sigma Aldrich, ≥ 99.9 %), which served as an OH scavenger (~ 440 times the initial α-pinene concentration), was injected into the chamber. Based on the cyclohexane and α-pinene concentrations in the chamber, the reaction rate of OH with cyclohexane is ~ 60 times greater than that with α-pinene. Ammonium sulfate (AS) seed aerosol was next introduced into the chamber via atomization of an aqueous AS solution. A known concentration of α-pinene (Sigma Aldrich, >99 %) (~ 50 ppb in all experiments) was then injected into the chamber. Finally, 500 ppb of ozone (O_3), which was generated by passing purified air into a photochemical cell (Jelight 610), was introduced into the chamber for 54.25 min after the seed aerosol and α-pinene concentrations in the chamber had stabilized. The beginning of O_3 injection into the chamber marked the start of the reaction (i.e., reaction time = 0 min). The O_3 mixing timescale was ~ 12 min for all experiments. The O_3 injection time and mixing timescale were determined from separate O_3-only experiments (Nah et al., 2016). In seed-only experiments performed to measure size-dependent particle-wall deposition coefficients, only AS seed aerosol was introduced into the chamber. A gas chromatograph-flame ionization detector (GC-FID, Agilent 7890A) and O_3 monitor (Teledyne T400) measured the α-pinene and O_3 concentrations, respectively. GC-FID measurements were taken 15 min apart. A high-resolution time-of-flight aerosol mass spectrometer (HR-ToF-AMS, Aerodyne Research Inc.) measured the aerosol elemental composition (DeCarlo et al., 2006; Canagaratna et al., 2015). A scanning mobility particle sizer (SMPS, TSI), which consists of a differential mobility analyzer (DMA, TSI 3081) and a condensation particle counter (CPC, TSI 3775), measured the aerosol size distributions, number and volume concentrations.

The initial total AS seed aerosol surface area concentrations used in this study were ~ 1000 and $\geq 8000\,\mu m^2\,cm^{-3}$ (referred to as "low-SA" and "high-SA" experiments, respectively). To investigate how the seed aerosol size distribution may affect SOA mass concentrations and yields, two different concentrations of AS solutions were used to generate AS seed aerosol for both the seed-only and α-pinene ozonolysis experiments: 0.015 or 0.05 M. In some experiments, both the 0.015 and 0.05 M AS solutions were atomized into the chamber to achieve the desired total AS seed aerosol surface area concentration. In these experiments, the 0.015 M AS solution was first atomized into the chamber to achieve about half of the desired total AS seed aerosol surface area concentration, followed by atomization of the 0.05 M AS solution. A summary of the experimental conditions is shown in Table 1.

3 Aerosol dynamics model

An aerosol dynamics model is used to determine particle-wall deposition coefficients that have been corrected for coagulation. This model was first described in Pierce et al. (2008). In our work, we do not use the full Aerosol Parameter Estimation (APE) model described in Pierce et al. (2008), but rather we employ the model used to create the "no condensation" curve in Fig. 5 of the paper. This model includes only coagulation and particle-wall loss, and it assumes that no condensation or evaporation occurs during seed-only experiments, which are especially designed to measure particle-wall deposition rates (experiments 1 through 6 in Table 1). Coagulation coefficients are calculated from Table 13.1 in Seinfeld and Pandis (2016). The inputs to the model are the raw time-dependent number distribution data measured by the SMPS during a particular seed-only experiment. For each time step of the SMPS measurements, the

Table 1. Experimental conditions and results.

Experiment	Experimental conditions	Initial seed aerosol surface area ($\mu m^2\ cm^{-3}$)	Initial [α-pinene][a] ($\mu g\ m^{-3}$)	ΔM_o[b,c] ($\mu g\ m^{-3}$)	SOA mass yield[d] (%)
1	0.015 M AS, seed only[e]	1090	–	–	–
2	0.05 M AS, seed only[e]	1190	–	–	–
3	0.015 M and 0.05 M AS, seed only[e]	1470	–	–	–
4	0.015 M and 0.05 M AS, seed only[e]	1210	–	–	–
5	0.05 M AS, seed only[f]	8000	–	–	–
6	0.015 M and 0.05 M AS, seed only[f]	8580	–	–	–
7	0.015 M AS, $O_3 + \alpha$-pinene[g,i]	1090	281.8 ± 14.9	71.5 ± 0.5	25.4 ± 1.3
8	0.05 M AS, $O_3 + \alpha$-pinene[g,j]	1260	278.5 ± 13.9	65.9 ± 0.9	23.7 ± 1.2
9	0.05 M AS, $O_3 + \alpha$-pinene[h,k]	9160	283.8 ± 14.2	74.2 ± 1.9	26.1 ± 1.5
10	0.05 M AS, $O_3 + \alpha$-pinene[h,k]	8390	265.8 ± 13.3	71.0 ± 3.4	26.7 ± 1.9
11	0.015 M and 0.05 M AS, $O_3 + \alpha$-pinene[h,l]	8180	289.8 ± 14.5	60.5 ± 1.7	20.9 ± 1.2
12	0.015 M and 0.05 M AS, $O_3 + \alpha$-pinene[h,l]	9440	271.8 ± 13.6	53.7 ± 2.9	19.7 ± 1.4

[a] All the α-pinene reacted in the 500 ppb O_3 experiments. [b] The SOA mass concentration (ΔM_o) is calculated using the density = 1.37 g cm^{-3} obtained from the 500 ppb O_3 nucleation experiment in Nah et al. (2016). [c] Uncertainties in the peak SOA mass concentration are calculated from 1 standard deviation of the aerosol volume as measured by the scanning mobility particle sizer. [d] SOA mass yields at peak SOA growth are reported. [e] Referred to as a low-SA seed-only experiment in the main text. [f] Referred to as a high-SA seed-only experiment in the main text. [g] Referred to as a low-SA experiment in the main text. [h] Referred to as a high-SA experiment in the main text. [i] Size-dependent particle-wall deposition coefficients obtained from experiment 1 were used for particle-wall deposition correction. [j] Size-dependent particle-wall deposition coefficients obtained from experiment 2 were used for particle-wall deposition correction. [k] Size-dependent particle-wall deposition coefficients obtained from experiment 5 were used for particle-wall deposition correction. [l] Size-dependent particle-wall deposition coefficients obtained from experiment 6 were used for particle-wall deposition correction.

model calculates the decrease in the number concentration in each particle size bin due solely to coagulation. The difference between this calculated decrease and the observed decrease in the number concentration is attributed to particle-wall deposition, thus allowing size-dependent particle-wall deposition coefficients to be determined. The model then recalculates the decrease in the number concentration for each particle size bin for that time step due to both coagulation and particle-wall deposition using the deposition coefficients just determined. The calculated decrease in the number concentration is again compared to the measured values. This process of finding the size-dependent particle-wall deposition rates is iterated using Newton's method until the calculated particle-wall deposition coefficients converge towards values where the calculated number concentration decay fits the observed decay. The process is repeated for each SMPS measurement time step, yielding size- and time-dependent particle-wall deposition coefficients. This process of finding the size-dependent particle-wall deposition rates is carried out only when the number concentration in the particle size bin of interest is > 20 particles cm^{-3}. For bins with ≤ 20 particles cm^{-3}, the deposition coefficient is not calculated during these time steps due to uncertainties in the number counts in these bins leading to low confidence in the determined particle-wall deposition rates. The deposition coefficients are averaged over the entire experiment to yield coagulation-corrected size-dependent particle-wall deposition coefficients.

4 Results and discussion

4.1 Role of coagulation in particle-wall deposition corrections

We performed a set of seed-only experiments using 0.015 M AS and/or 0.05 M AS solutions to determine the extent to which size-dependent particle-wall loss rates change with different seed aerosol concentrations and size distributions (experiments 1 through 6 in Table 1). The initial total AS seed aerosol surface area concentrations in the low-SA seed-only and high-SA seed-only experiments are similar to those used in the α-pinene ozonolysis experiments (i.e., ~ 1000 and $\geq 8000\ \mu m^2\ cm^{-3}$, respectively). Figure S1 in the Supplement shows the initial and final (420 min) number and volume size distributions for the seed-only experiments. The initial number and volume size distributions in the low-SA seed-only experiments are smaller than those in the high-SA seed-only experiments, regardless of the concentration of the AS solution used to generate seed aerosol. As expected, all of the size distributions shift to larger particle diameters as the experiment progresses due to more efficient loss of smaller particles to the chamber walls and via coagulation as compared to larger particles.

Figure 1 shows the size-dependent particle-wall deposition coefficients measured directly in the low-SA seed-only and high-SA seed-only experiments (dashed lines). We will refer to them as the *uncorrected* size-dependent particle-wall deposition coefficients for the remainder of the dis-

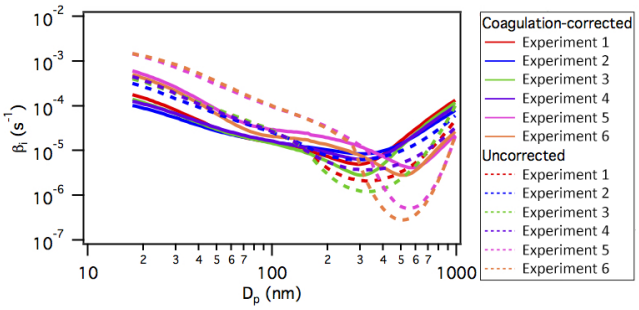

Figure 1. Uncorrected (dashed lines) and coagulation-corrected (solid lines) particle-wall deposition coefficients (β_i) for the low-SA seed-only (experiments 1 through 4) and high-SA seed-only (experiments 5 and 6) experiments. Refer to Table 1 for information on the AS solution(s) used to generate the seed aerosol and the initial seed aerosol surface area concentrations in these experiments.

cussion in this work since the effect of coagulation is assumed to be negligible, and thus coagulation is not corrected for in these coefficients. The uncorrected size-dependent particle-wall deposition coefficients are obtained directly from SMPS measurements by fitting a first-order exponential decay to the measured particle number concentration decay in each size bin. The uncorrected particle-wall deposition coefficients are compared to those corrected for coagulation (shown as solid lines in Fig. 1), which are obtained from the application of the aerosol dynamics model (described in Sect. 3) to the number distribution data measured by the SMPS. As anticipated, a comparison of the uncorrected and coagulation-corrected size-dependent particle-wall deposition coefficients indicates that coagulation has a smaller effect on the deposition coefficients from the low-SA seed-only experiments (experiments 1 through 4) compared to the high-SA seed-only experiments (experiments 5 and 6). For example, for particle diameters >400 nm, the coagulation-corrected deposition coefficients for the high-SA seed-only experiments are up to 1 order of magnitude faster than the uncorrected deposition coefficients. The smaller uncorrected deposition coefficients can be attributed to particle formation (via coagulation) occurring simultaneously with particle-wall deposition at these larger particle diameters in the high-SA seed-only experiments. A comparison of the change in total particle number concentration due to coagulation alone (Fig. S2) shows that the low-SA seed-only experiments (experiments 1 through 4) have smaller coagulation rates than the high-SA seed-only experiments (experiments 5 and 6). The observation that coagulation has a smaller effect on the inferred deposition coefficients in the low-SA seed-only experiments is expected since these experiments involve significantly smaller particle number concentrations as compared to the high-SA seed-only experiments (2.5 to 4×10^4 particles cm^{-3} vs. 1 to 1.3×10^5 particles cm^{-3}).

The coagulation-corrected size-dependent particle-wall deposition coefficients obtained from the low-SA seed-only experiments are generally in agreement. This is also the case for the coagulation-corrected particle-wall deposition coefficients obtained from the high-SA seed-only experiments. Similar trends are observed for the uncorrected size-dependent particle-wall deposition coefficients. Therefore, the concentration of the AS solution(s) (i.e., 0.015 M and/or 0.05 M) used to generate the seed aerosol in seed-only experiments does not influence the size-dependent particle-wall deposition coefficients. The coagulation-corrected size-dependent particle-wall deposition coefficients obtained from the low-SA seed-only experiments are different from those obtained from the high-SA seed-only experiments. In addition, the minimum coagulation-corrected particle-wall deposition coefficient for the low-SA seed-only experiment (minimum particle diameter ∼300 nm) is lower than that of the high-SA seed-only experiments (minimum particle diameter ∼530 nm). This result is surprising since the particle-wall deposition coefficients are expected to depend solely on particle size once coagulation is accounted for.

We identify two possible explanations for the differences in the coagulation-corrected particle-wall deposition coefficients. The first possibility is that there is a difference in particle charging of the seed aerosol in the low-SA seed-only and high-SA seed-only experiments. Particle-wall deposition is enhanced when charges are present on particles (McMurry and Grosjean, 1985; McMurry and Rader, 1985; Pierce et al., 2008). In all of our experiments, a Boltzmann charge distribution was applied to the AS seed aerosol by passing the particles through a Po-210 neutralizer prior to injection into the chamber. However, it is possible that the particles are not fully neutralized before entering the chamber, resulting in a difference in the true particle-wall deposition coefficients due to the differences in particle charging between the experiments.

The second possible explanation for the differences in the coagulation-corrected particle-wall deposition coefficients is that the Brownian coagulation kernel that we used for our coagulation correction may not account for the entire coagulation rate in the chamber. Coulombic and/or van der Waals forces may enhance the coagulation rates. We performed a series of sensitivity tests to determine the extent to which the coagulation-corrected size-dependent particle-wall deposition coefficients change as a function of coagulation coefficients. In these tests, we scale the Brownian coagulation kernel by 1.1 and 1.5 uniformly across all particle sizes (since Coulombic and van der Waals enhancements to coagulation have size dependence, these simple sensitivity tests do not fully capture the changes due to either of these forces). Figure S3 shows results from sensitivity tests performed on the seed-only experiments. These sensitivity tests show that the coagulation-corrected particle-wall deposition coefficients in the low-SA seed-only and high-SA seed-only experiments converge towards each other with increasing

scale factors on coagulation. However, with increasing coagulation scale factors, our derived wall deposition coefficients become negative at some particle sizes, which implies that the size-independent coagulation scale factors are unrealistic. Future work should include a more detailed investigation of the size-dependent coagulation enhancements provided by Coulombic and van der Waals forces (which in turn requires knowledge about the charge distribution and van der Waals forces), and it should include an investigation of the charge-enhanced particle-wall losses (again requiring a knowledge of the charge distribution). For the remainder of this work, we will use coagulation-corrected particle-wall deposition coefficients with no enhancement to the coagulation rates (solid lines in Figs. 1 and S3a).

We evaluated the effectiveness of the coagulation-corrected particle-wall deposition coefficients (with no scaling of Brownian coagulation) in correcting for particle-wall loss and coagulation by applying these coefficients to the SMPS data from the seed-only experiments. The corrected volume concentration should level off at a constant value (at the initial particle volume concentration) when particle-wall deposition and coagulation are properly accounted for since no condensation or evaporation occurs during these experiments (due to the use of low-volatility AS seed aerosol and the absence of condensable gases) and the wall-deposited particle volume concentration is added back to the suspended particle volume concentration during particle-wall loss correction. Figure S4 shows the raw and particle-wall-deposition-corrected volume concentrations. Coagulation-corrected size-dependent particle-wall deposition coefficients are used for the particle-wall deposition correction shown in Fig. S4. Over all experiments, the particle-wall-deposition-corrected final volume concentration (i.e., at the end of the experiment) is within 1 to 5 % of the initial volume concentration (Table S1).

4.2 α-pinene ozonolysis

We use the "size-dependent" method described in Loza et al. (2012) and Nah et al. (2016) to correct for particle-wall deposition in the α-pinene ozonolysis experiments. Briefly, size-dependent particle-wall deposition coefficients determined in separate seed-only experiments (either through direct measurements or using an aerosol dynamics model) are used to correct for particle-wall deposition in SOA formation experiments. Here we assume that particles cease to uptake SOA-forming vapors once they have deposited, and hence the SOA mass present on deposited particles does not increase after deposition. A key assumption of the size-dependent method is that the size-dependent particle-wall deposition coefficients do not change significantly between experiments. Seed-only experiments are performed regularly in the GTEC chamber. As shown in Fig. 1 (and Fig. 1 of Nah et al., 2016), the uncorrected and coagulation-corrected size-dependent particle-wall deposition coefficients are generally in line with each other at a given seed aerosol surface area concentration. Since the seed-only and α-pinene ozonolysis experiments were performed under similar experimental conditions (i.e., dark conditions at < 5 % RH and 25 °C), the size-dependent particle-wall deposition coefficients are not expected to change significantly with reaction conditions for the experiments presented in this study.

Since the focus of this work is the influence of coagulation and particle-wall deposition on SOA mass yields, more high-SA α-pinene ozonolysis experiments (experiments 9 through 12) were performed than low-SA experiments (experiments 7 and 8). To investigate the influence of coagulation on the SOA mass yields, both the uncorrected and coagulation-corrected size-dependent particle-wall deposition coefficients are used to correct for particle-wall deposition in the α-pinene ozonolysis experiments. All the low-SA α-pinene ozonolysis data are particle-wall-deposition corrected using uncorrected and coagulation-corrected size-dependent particle-wall deposition coefficients from the low-SA seed-only experiments, and all the high-SA α-pinene ozonolysis data are corrected using uncorrected and coagulation-corrected particle-wall deposition coefficients from the high-SA seed-only experiments. Additional details regarding the size-dependent particle-wall deposition coefficients used to correct for particle-wall deposition in the different α-pinene ozonolysis experiments are provided in Table 1. Figure S5 shows the raw and particle-wall-deposition-corrected aerosol volume concentrations for all the α-pinene ozonolysis experiments. In all the α-pinene ozonolysis experiments, the volume concentrations that were particle-wall-deposition corrected using coagulation-corrected size-dependent particle-wall deposition coefficients (black) reach peak values at reaction time ∼ 100 min. In contrast, volume concentrations that were particle-wall-deposition corrected using uncorrected size-dependent particle-wall deposition coefficients (blue) increase monotonically in the high-SA experiments (experiments 9 through 12).

The SOA mass concentration is calculated from the product of the SOA density with the difference of the particle-wall-deposition-corrected volume concentration and the initial seed aerosol volume concentration. We use an SOA density of 1.37 g cm^{-3}, which was previously measured by Nah et al. (2016). Figure 2 shows the reaction profiles of the low-SA α-pinene ozonolysis experiments. The SOA mass concentrations obtained using the coagulation-corrected (Fig. 2a and b) and uncorrected (Fig. 2c and d) size-dependent particle-wall deposition coefficients are sufficiently similar, which suggests that coagulation plays a minor role in the low-SA experiments. As reported in Nah et al. (2016), SOA growth typically occurs within 10 to 20 min of the start of the reaction. The molar ratio of O_3 reacted to α-pinene reacted is approximately 1 : 1 (i.e., 50 ppb α-pinene reacted with 50 ppb O_3), which indicates that O_3 reacts with α-pinene and not its oxidation products. All of the α-pinene reacts within 90 to 100 min after the start of the reaction in the 500 ppb O_3

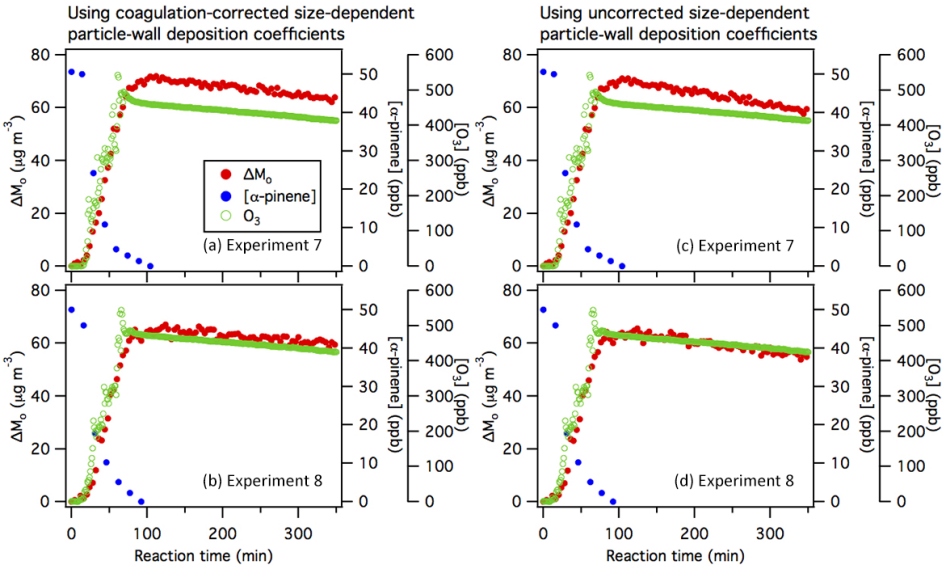

Figure 2. Reaction profiles of the low-SA α-pinene ozonolysis experiments. Panels **(a)** and **(b)** show SOA mass concentrations (ΔM_o) obtained using the coagulation-corrected size-dependent particle-wall deposition coefficients from the low-SA seed-only experiments, while panels **(c)** and **(d)** show SOA mass concentrations (ΔM_o) obtained using the uncorrected size-dependent particle-wall deposition coefficients from the low-SA seed-only experiments. Refer to Table 1 for information on the AS solution(s) used to generate the seed aerosol and the initial seed aerosol surface area concentrations in these experiments.

experiments, and peak SOA levels occur at reaction time ~ 100 min. SOA growth basically ceases once all the α-pinene has reacted, indicating that the first step of α-pinene ozonolysis is rate limiting and the first-generation products are condensable (Gao et al., 2004a, b; Ng et al., 2006; Chan et al., 2007). This result is expected since α-pinene has a single double bond. The slight decrease in the SOA mass concentrations after peak SOA growth may be due to imperfections in the particle-wall deposition correction and/or vapor-wall deposition.

Figure 3 shows the reaction profiles of the high-SA α-pinene ozonolysis experiments. In cases where the coagulation-corrected size-dependent particle-wall deposition coefficients are used to correct for particle-wall deposition (Fig. 3a–d), the SOA growth profile is similar to that of the low-SA experiments; SOA growth essentially stops once all the α-pinene has reacted, as expected (Gao et al., 2004a, b; Ng et al., 2006; Chan et al., 2007). In contrast, when the uncorrected size-dependent particle-wall deposition coefficients are used to correct for particle-wall deposition (Fig. 3e–h), the SOA mass concentration continues to increase even after all the α-pinene has reacted. This indicates that for the size-dependent method, SOA mass concentrations, and consequently SOA mass yields, can be substantially overestimated when coagulation is not accounted for during particle-wall deposition correction in high-SA experiments. This underscores the importance of accounting for coagulation and particle-wall deposition appropriately in chamber studies that employ high seed aerosol concentrations. We use SOA mass concentrations corrected using coagulation-corrected size-dependent particle-wall deposition coefficients (solid lines in Fig. 1) for the remainder of the discussion in this work.

Figure 4 shows the time-dependent SOA mass yields as a function of initial seed aerosol surface area concentration for the α-pinene ozonolysis experiments. Also included in Fig. 4 are results from Nah et al. (2016); SOA mass concentrations were obtained using coagulation-corrected size-dependent particle-wall deposition coefficients determined in their study (Fig. S7 of Nah et al., 2016). The SOA mass yield at peak SOA growth remains approximately constant even at seed aerosol surface area concentrations $\geq 8000\,\mu m^2\,cm^{-3}$. This confirms conclusions from our previous study that the seed aerosol surface area concentration does not influence the partitioning of gas-phase products to the particle phase in the α-pinene ozonolysis system (Nah et al., 2016). As discussed in Nah et al. (2016), this behavior arises because SOA formation in the α-pinene ozonolysis system is dominated by quasi-equilibrium growth (Saleh et al., 2013), which occurs when the production rate of SOA-forming vapors is significantly slower than that required to establish gas-particle equilibrium (Riipinen et al., 2011; Shiraiwa and Seinfeld, 2012; Zhang et al., 2012). Gas-particle equilibrium is governed by the amount of organic material in the system when the vapor and particle phases maintain equilibrium. Thus, the seed aerosol surface area does not control the condensation rate of SOA-forming vapors (McVay et al., 2014).

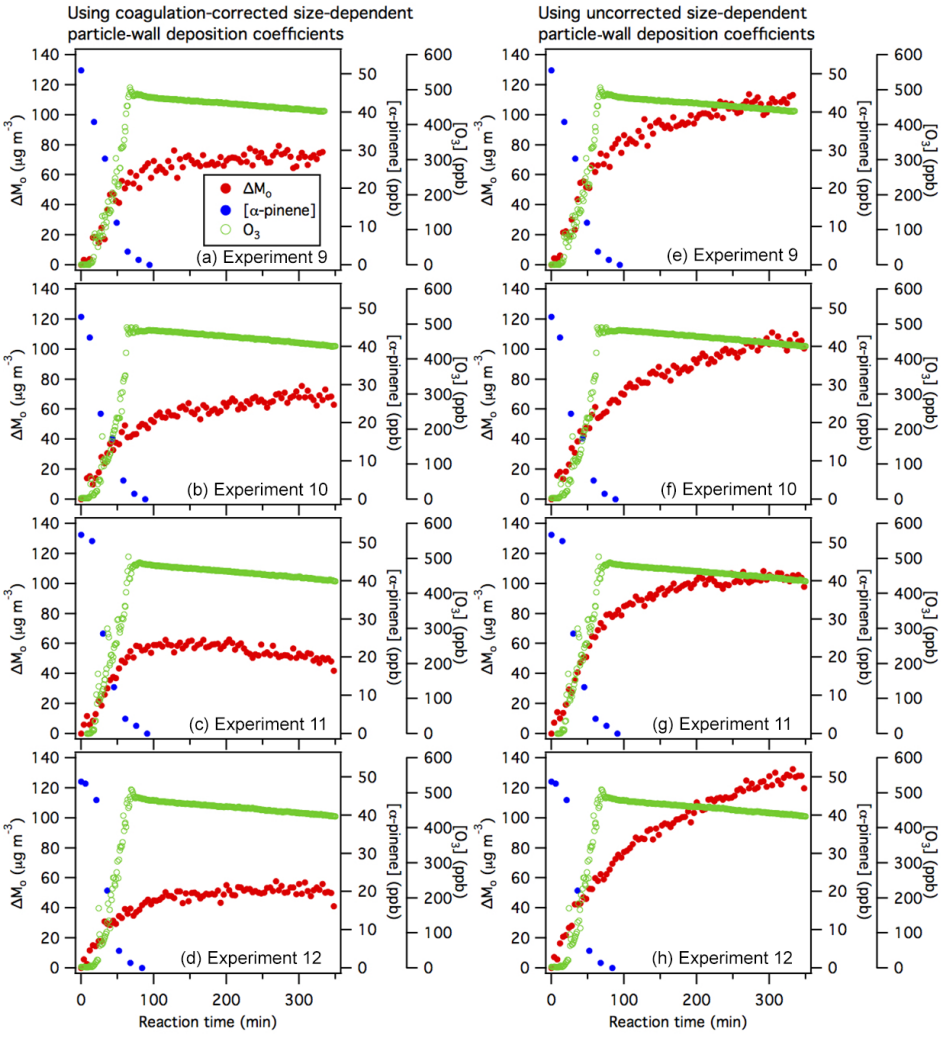

Figure 3. Reaction profiles of the high-SA α-pinene ozonolysis experiments. Panels **(a–d)** show SOA mass concentrations (ΔM_o) obtained using the coagulation-corrected size-dependent particle-wall deposition coefficients from the high-SA seed-only experiments, while panels **(e–h)** show SOA mass concentrations (ΔM_o) obtained using the uncorrected size-dependent particle-wall deposition coefficients from the high-SA seed-only experiments. Refer to Table 1 for information on the AS solution(s) used to generate the seed aerosol and the initial seed aerosol surface area concentrations in these experiments. As explained in the main text, SOA mass concentrations are substantially overestimated when the uncorrected size-dependent particle-wall deposition coefficients are used to account for particle-wall deposition.

It is important to note that when the uncorrected size-dependent particle-wall deposition coefficients (dashed lines in Fig. 1) are used for the particle-wall deposition correction, the predicted SOA mass yield at peak SOA growth increases with seed aerosol surface area (Fig. S6). This trend would lead to the incorrect conclusion that SOA formation in the α-pinene ozonolysis system is governed by kinetically limited growth. Therefore, this result further highlights the importance of accounting for coagulation and particle-wall deposition properly in chamber studies (especially when high number concentrations of seed aerosol are used) to avoid erroneous conclusions regarding the role of gas-particle partitioning (quasi-equilibrium vs. kinetically limited SOA growth) in affecting vapor-wall deposition and SOA mass yields in VOC systems.

4.3 Uncertainties in SOA mass concentrations due to particle-wall loss corrections

In the previous section, we showed that ignoring the role of coagulation in the size-dependent particle-wall deposition correction method can contribute significant errors to the calculated SOA mass concentrations and yields. These uncertainties could lead to erroneous conclusions regarding the role of gas-particle partitioning in influencing vapor-wall loss in the VOC system. Here, we investigate the uncertainties in the SOA mass concentrations and yields as a result of the

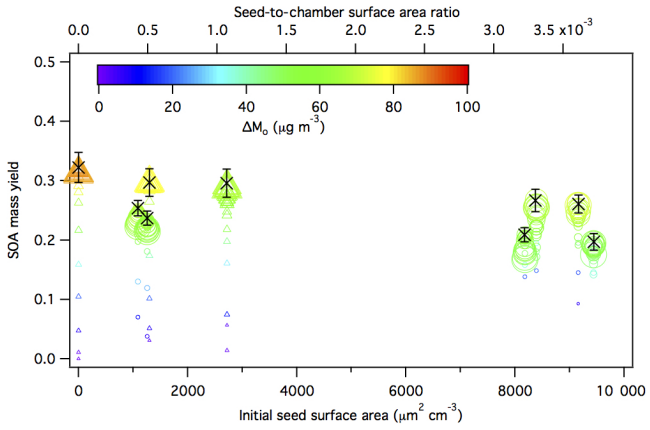

Figure 4. Averaged SOA mass yields over the course of an α-pinene ozonolysis experiment as a function of initial total AS seed aerosol surface area concentration. Results from this study (15 min averaged) are shown as circles, while results from the study by Nah et al. (2016) (10 min averaged) are shown as triangles. All the SOA mass yields shown here (including results from Nah et al., 2016) are obtained using the coagulation-corrected size-dependent particle-wall deposition coefficients. Symbol color indicates the SOA mass concentration and symbol size indicates the time after O_3 is injected into the chamber. The $\times$ symbols are the SOA mass yields at peak SOA growth obtained from the experimental data. The y axis error bars represent the uncertainty in the SOA mass yield at peak SOA growth, which originates from the α-pinene injection and the aerosol mass concentration at peak SOA growth (1 standard deviation).

use of different particle-wall deposition correction methods. We analyzed data from the α-pinene ozonolysis experiments using four different commonly used particle-wall deposition correction methods. SOA mass concentrations and yields obtained using the size-dependent particle-wall deposition correction method (discussed in Sect. 4.2) are compared to those obtained using the "number-averaged", "volume-averaged" and "inert tracer" methods, which were described previously by Carter et al. (2005), Pathak et al. (2007) and Hildebrandt et al. (2009), respectively. For the size-dependent method, only SOA mass concentrations and yields corrected using coagulation-corrected size-dependent particle-wall deposition coefficients (Fig. 4) are used in the discussion presented here.

The number-averaged and volume-averaged methods use SMPS measurements taken during SOA formation studies. The number-averaged method involves measuring the average loss rate of the total aerosol number concentration after peak SOA growth and then applying this first-order particle-wall deposition rate to the entire experiment to correct for particle-wall loss (Carter et al., 2005). Since the average loss rate of the total aerosol volume concentration is assumed to be the same as that of the total aerosol number concentration, this first-order particle-wall deposition rate is also applied to the total aerosol volume concentration data to determine the SOA mass concentration. The volume-averaged method involves measuring the average loss rate of the total aerosol volume or mass concentration after peak SOA growth, and then applying this first-order particle-wall deposition rate to the entire experiment to correct for particle-wall loss (Pathak et al., 2007). Since the particle-wall deposition rate is directly measured during SOA formation experiments in the number-averaged and volume-averaged methods, day-to-day variations of the particle-wall deposition rates are accounted for. Unlike the size-dependent method, the number-averaged and volume-averaged methods assume that particle-wall deposition rates depend weakly on particle size, and hence particle-wall deposition can be represented by a single first-order decay rate constant (Carter et al., 2005; Pathak et al., 2007; Pierce et al., 2008). It is currently unclear if this assumption is valid for all seed aerosol concentrations (i.e., number, surface area and volume concentrations). The inert tracer method can be used in SOA formation studies where SMPS and AMS measurements are taken and nonvolatile sulfate seed aerosol is used (Hildebrandt et al., 2009). The SOA mass concentration is calculated from the product of the initial seed aerosol sulfate mass concentration (measured by the SMPS) to the time-dependent organic-to-sulfate (Org / SO_4) ratio (measured by the HR-ToF-AMS). Examples of the application of the number-averaged, volume-averaged and inert tracer methods to the α-pinene ozonolysis data are shown in Fig. S7.

In original descriptions of the size-dependent, number-averaged and volume-averaged methods, the authors assumed that particles cease to uptake SOA-forming vapors once they have deposited to the walls; thus, the SOA mass present on deposited particles does not increase after deposition (Carter et al., 2005; Pathak et al., 2007; Loza et al., 2012). In contrast, the inert tracer method assumes that deposited particles continue to uptake suspended SOA-forming vapors at similar rates as suspended particles, and hence the SOA mass present on the deposited particles will increase at the same rate as those suspended (Hildebrandt et al., 2009). Therefore, SOA mass concentrations and yields calculated by the inert tracer method are expected to be higher than that calculated using the original descriptions of the size-dependent, number-averaged and volume-averaged methods. It is important to note that the assumption that deposited particles continue to uptake suspended SOA-forming vapors at similar rates as suspended particles can also be applied to the size-dependent, number-averaged and volume-averaged methods, which in turn will result in higher calculated SOA mass concentrations and yields. However, we use the size-dependent, number-averaged and volume-averaged methods as originally described by Loza et al. (2012), Carter et al. (2005) and Pathak et al. (2007), respectively, to correct for particle-wall deposition in this discussion (i.e., deposited particles do not uptake SOA-forming vapors). The inert tracer method will be used to evaluate its ability to predict the role of gas-particle partitioning (quasi-equilibrium

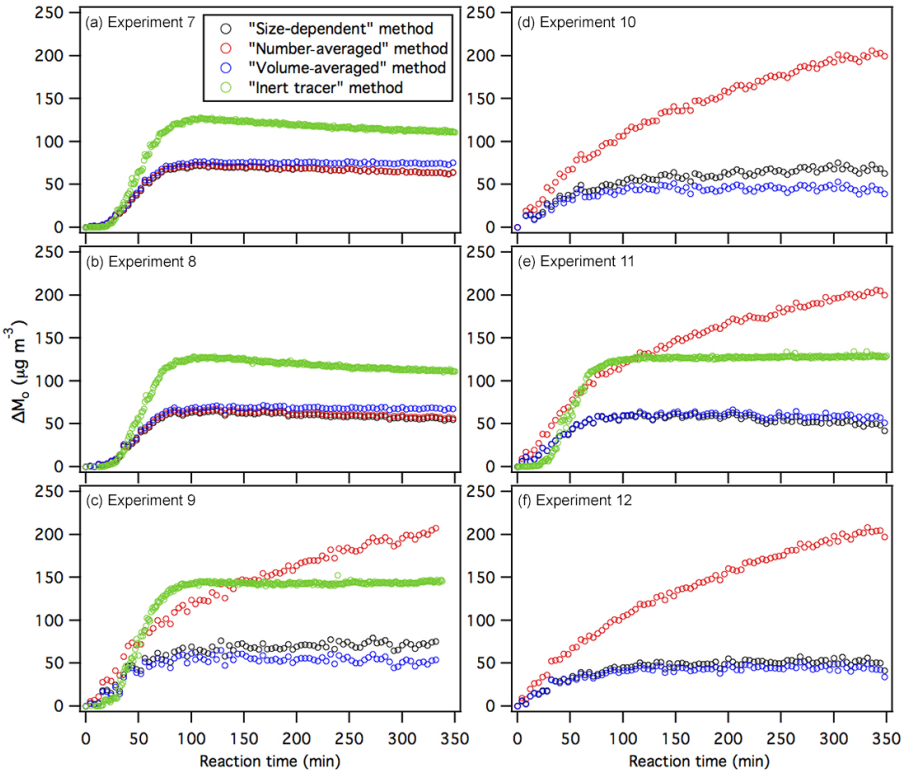

Figure 5. SOA mass concentration (ΔM_o) as a function of reaction time in the α-pinene ozonolysis experiments using the size-dependent, number-averaged, volume-averaged and inert tracer particle-wall deposition correction methods. HR-ToF-AMS data were not available in experiments 10 and 12; therefore, SOA mass concentrations calculated using the inert tracer method were not available in these experiments.

vs. kinetically limited SOA growth) in affecting vapor-wall deposition and SOA mass yields in the α-pinene ozonolysis system.

Figure 5 shows the SOA mass concentrations as a function of reaction time for the four particle-wall deposition correction methods. For the low-SA experiments (Fig. 5a and b), the SOA growth profiles obtained using the four different particle-wall deposition correction methods are similar; SOA growth virtually stops after all the α-pinene has reacted (at reaction time $\sim$90 to 100 min). As expected, the SOA mass concentrations calculated by the inert tracer method are higher than the SOA mass concentrations calculated by the size-dependent, number-averaged and volume-averaged methods. The SOA mass concentrations calculated by the size-dependent, number-averaged and volume-averaged particle-wall deposition methods are generally consistent with each other.

For the high-SA experiments (Fig. 5c to f), the SOA mass concentrations calculated using the size-dependent, volume-averaged and inert tracer methods stop increasing after all the α-pinene has reacted (at reaction time $\sim$90 to 100 min). In contrast, the SOA mass concentrations calculated using the number-averaged method continued to increase even after all the α-pinene was reacted. These results suggest that the calculated SOA mass concentrations and yields will be substantially overestimated if the number-averaged method is used to correct for particle-wall deposition in experiments where high seed aerosol surface area concentrations are used. The erroneous increase in the SOA mass concentration calculated by the number-averaged method can be attributed to the method's assumption that the average loss rate of the total aerosol volume concentration is the same as that of the total aerosol number concentration. The number-averaged method is effective in experiments where low concentrations of seed aerosol are used since coagulation plays a minor role in affecting the average loss rate of the total aerosol number concentration. However, it loses its accuracy in experiments under high seed aerosol number concentrations because the average loss rate of the total aerosol number concentration is driven by both coagulation and particle-wall deposition. It is possible that the number-averaged method may be an effective particle-wall deposition correction method in these experiments if the measurements are corrected for coagulation. The effect of coagulation on the SOA mass concentrations calculated by the volume-averaged and inert tracer methods is less prominent since coagulation does not affect the aerosol volume and mass concentrations. Together, our results indicate that the size-dependent (when coagulation is accounted for), volume-averaged and inert tracer methods are effective particle-wall deposition correction methods (regardless

of seed aerosol surface area concentrations) since the calculated SOA mass concentrations stopped increasing after all the α-pinene had reacted.

Figure 6 shows the time-dependent SOA mass yields as a function of initial total AS seed aerosol surface area concentration for the number-averaged, volume-averaged and inert tracer particle-wall deposition correction methods. Also shown in Fig. 6 are time-dependent SOA mass yields calculated using these three methods for the α-pinene ozonolysis raw data reported by Nah et al. (2016). The time-dependent SOA mass yields for the number-averaged, volume-averaged and inert tracer methods (Fig. 6) are compared to those calculated using the size-dependent method (Fig. 4). For seed aerosol surface area concentrations $< 3000\,\mu m^2\,cm^{-3}$, the SOA mass yields at peak SOA growth (absolute values) calculated by the size-dependent, number-averaged and volume-averaged methods agree within 14 % (Figs. 4, 6a and b). In contrast, for seed aerosol surface area concentrations $\geq 8000\,\mu m^2\,cm^{-3}$, the SOA mass yields at peak SOA growth calculated by the number-averaged method range from 70.8 to 76.5 % (Fig. 6a), while SOA mass yields at peak SOA growth calculated by the size-dependent and volume-averaged methods range from 17.2 to 27 % (Figs. 4 and 6b). As discussed previously, this disagreement in the SOA mass yields is due to the treatment (or lack thereof) of coagulation in the number-averaged method. Failure to account for coagulation in the number-averaged method also resulted in the calculated SOA mass yields increasing with seed aerosol surface area (Fig. 6a), which could lead to the incorrect conclusion that SOA formation in the α-pinene ozonolysis system is governed by kinetically limited growth. In contrast, the SOA mass yields calculated by the volume-averaged and inert tracer methods remain roughly constant despite the increase in AS seed aerosol surface area (Fig. 6b and c), which is consistent with the results obtained using the size-dependent method (Fig. 4).

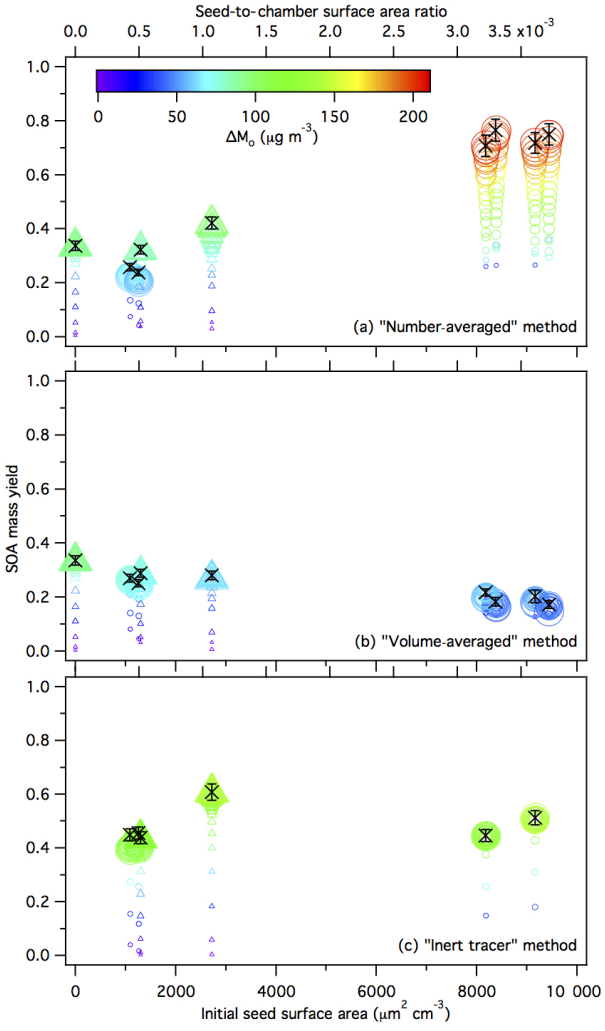

Figure 6. Averaged SOA mass yields over the course of an α-pinene ozonolysis experiment as a function of initial total AS seed aerosol surface area concentration using the **(a)** number-averaged, **(b)** volume-averaged and **(c)** inert tracer particle-wall deposition correction methods. Results from this study (15 min averaged) are shown as circles, while results from the study by Nah et al. (2016) (10 min averaged) are shown as triangles. Symbol color indicates the SOA mass concentration and symbol size indicates the time after O_3 is injected into the chamber. The $\times$ symbols are the SOA mass yields at peak SOA growth obtained from the experimental data. The y axis error bars represent the uncertainty in the SOA mass yield at peak SOA growth, which originates from the α-pinene injection and the aerosol mass concentration at peak SOA growth (1 standard deviation).

5 Conclusions

An aerosol dynamics model can be used to account for coagulation in chamber studies in which large seed aerosol surface area concentrations are used. Coagulation-corrected size-dependent particle-wall deposition coefficients are obtained from the application of the aerosol dynamics model to the experimental data from seed-only experiments. Using these coagulation-corrected size-dependent particle-wall deposition coefficients, we showed that the α-pinene ozonolysis SOA mass yields at peak SOA growth remain approximately constant even when very high seed aerosol surface area concentrations ($\geq 8000\,\mu m^2\,cm^{-3}$) are used. This confirms conclusions from our previous study that the seed aerosol surface area concentration does not influence the partitioning of α-pinene ozonolysis gas-phase products to the particle phase (Nah et al., 2016). Thus, this indicates that SOA formation in the α-pinene ozonolysis system is dominated by quasi-equilibrium growth and that there are no significant limitations to vapor-particle mass transfer (McVay et al., 2014; Nah et al., 2016).

The variability in the calculated SOA mass concentrations and yields between four different particle-wall deposition correction methods is also evaluated for a series of α-

pinene ozonolysis experiments. In the experiments with low seed aerosol surface area concentrations ($< 3000\,\mu m^2\,cm^{-3}$), the SOA mass yields obtained by the different particle-wall deposition correction methods (i.e., the size-dependent, number-averaged and volume-averaged methods) are generally consistent with one another. This indicates that these three methods are effective in correcting for particle-wall deposition in experiments that use low seed aerosol surface area concentrations. However, in the experiments with high seed aerosol surface area concentrations ($\geq 8000\,\mu m^2\,cm^{-3}$), the calculated SOA mass yields differ substantially. These differences arise from assumptions made in the particle-wall deposition correction method regarding the influence of coagulation on the first-order particle-wall loss rate. Specifically, we find that coagulation needs to be accounted for in the size-dependent and number-averaged methods in order for them to be effective in chamber studies that use high seed aerosol surface area concentrations. Coagulation does not need to be accounted for in the volume-averaged method since coagulation does not affect aerosol volume concentrations.

Chamber experiments are subject to both particle and vapor-wall deposition. While understanding the effect of vapor-wall deposition on the SOA mass yields is critical, SOA mass yield uncertainties introduced by the particle-wall deposition correction cannot be neglected. Results from this study underscore the importance of constraining the SOA mass yield uncertainties introduced by the particle-wall deposition correction regardless of the VOC system. Specifically, the effect of coagulation on particle-wall deposition rates can be an important source of uncertainty not only in determining SOA mass concentrations and yields, but also in evaluating the role of gas-particle partitioning (quasi-equilibrium vs. kinetically limited SOA growth) in affecting vapor-wall deposition in VOC systems. Here we showed that the condensation of SOA-forming vapors in the α-pinene ozonolysis system can be erroneously concluded as kinetically limited if coagulation is not accounted for in the size-dependent and number-averaged particle-wall deposition correction methods. Similarly flawed conclusions in other VOC systems may be drawn in chamber studies that use high seed aerosol surface area concentrations to promote SOA formation but do not account for coagulation. Therefore, we recommend accounting for coagulation when the size-dependent and number-averaged particle-wall deposition correction methods are used in chamber studies that use high seed aerosol surface area concentrations (e.g., $\geq 3000\,\mu m^2\,cm^{-3}$) to promote the condensation of SOA-forming vapors onto seed aerosol regardless of VOC system. Alternatively, the volume-averaged and inert tracer methods can be used in chamber studies that use high seed aerosol surface area concentrations. In addition, we suggest using multiple techniques (i.e., at least two) to correct for particle-wall loss in order to determine the effect of SOA mass yield uncertainties introduced by particle-wall deposition correction. Complications arising from particle and vapor-wall deposition may also be potentially minimized by conducting shorter duration chamber experiments. This can be achieved by using excess oxidant concentrations, which increase the oxidation rate, and consequently reduce the time at which peak SOA growth is achieved (Nah et al., 2016).

It is important to note that while results from the present study indicate that the volume-averaged and inert tracer methods are appropriate particle-wall deposition correction methods for SOA formation studies (regardless of seed aerosol surface area concentrations) performed in the GTEC chamber in which the particle-wall loss rates strongly depend on particle size, this may not be the case for all chambers. In addition to particle size, particle-wall deposition rates depend on the chamber geometry, chamber turbulence induced by mixing and charge distribution on particles (Crump and Seinfeld, 1981; McMurry and Rader, 1985). All of these factors need to be considered before one decides which particle-wall deposition correction method to use in SOA formation studies. It is possible that the volume-averaged and inert tracer methods may not be appropriate particle-wall deposition correction methods for SOA formation studies performed in a chamber in which the particle-wall loss rates are even more strongly dependent on particle size compared to the GTEC chamber. Therefore, we recommend performing at least one separate seed-only experiment to measure the size-dependent particle-wall deposition coefficients in order to probe the particle-wall deposition characteristics of the chamber used before deciding on the particle-wall deposition method to use in SOA formation studies.

6 Data availability

The experimental data can be accessed by request (ng@chbe.gatech.edu).

The Supplement related to this article is available online at doi:10.5194/acp-17-2297-2017-supplement.

Competing interests. The authors declare that they have no conflict of interest.

Disclaimer. This publication's contents are solely the responsibility of the grantee and do not necessarily represent the official views of the US EPA. Furthermore, the US EPA does not endorse the purchase of any commercial products or services mentioned in the publication.

Acknowledgements. This research was funded by NSF grants 1455588 and AGS-1523500 and the US Environmental Protection Agency STAR grant (Early Career) RD-83540301. Renee C. McVay was supported by a National Science Foundation Graduate Research Fellowship under grant No. DGE-1144469.

Edited by: M. C. Facchini
Reviewed by: two anonymous referees

References

Boyd, C. M., Sanchez, J., Xu, L., Eugene, A. J., Nah, T., Tuet, W. Y., Guzman, M. I., and Ng, N. L.: Secondary organic aerosol formation from the β-pinene+NO_3 system: effect of humidity and peroxy radical fate, Atmos. Chem. Phys., 15, 7497–7522, doi:10.5194/acp-15-7497-2015, 2015.

Canagaratna, M. R., Jimenez, J. L., Kroll, J. H., Chen, Q., Kessler, S. H., Massoli, P., Hildebrandt Ruiz, L., Fortner, E., Williams, L. R., Wilson, K. R., Surratt, J. D., Donahue, N. M., Jayne, J. T., and Worsnop, D. R.: Elemental ratio measurements of organic compounds using aerosol mass spectrometry: characterization, improved calibration, and implications, Atmos. Chem. Phys., 15, 253–272, doi:10.5194/acp-15-253-2015, 2015.

Cappa, C. D., Jathar, S. H., Kleeman, M. J., Docherty, K. S., Jimenez, J. L., Seinfeld, J. H., and Wexler, A. S.: Simulating secondary organic aerosol in a regional air quality model using the statistical oxidation model – Part 2: Assessing the influence of vapor wall losses, Atmos. Chem. Phys., 16, 3041–3059, doi:10.5194/acp-16-3041-2016, 2016.

Carter, W. P. L., Cocker, D. R., Fitz, D. R., Malkina, I. L., Bumiller, K., Sauer, C. G., Pisano, J. T., Bufalino, C., and Song, C.: A new environmental chamber for evaluation of gas-phase chemical mechanisms and secondary aerosol formation, Atmos. Environ., 39, 7768–7788, doi:10.1016/j.atmosenv.2005.08.040, 2005.

Chan, A. W. H., Kroll, J. H., Ng, N. L., and Seinfeld, J. H.: Kinetic modeling of secondary organic aerosol formation: effects of particle- and gas-phase reactions of semivolatile products, Atmos. Chem. Phys., 7, 4135–4147, doi:10.5194/acp-7-4135-2007, 2007.

Cocker, D. R., Flagan, R. C., and Seinfeld, J. H.: State-of-the-art chamber facility for studying atmospheric aerosol chemistry, Environ. Sci. Technol., 35, 2594–2601, doi:10.1021/es0019169, 2001.

Crump, J. G. and Seinfeld, J. H.: Turbulent Deposition and Gravitational Sedimentation of an Aerosol in a Vessel of Arbitrary Shape, J. Aerosol Sci., 12, 405–415, doi:10.1016/0021-8502(81)90036-7, 1981.

DeCarlo, P. F., Kimmel, J. R., Trimborn, A., Northway, M. J., Jayne, J. T., Aiken, A. C., Gonin, M., Fuhrer, K., Horvath, T., Docherty, K. S., Worsnop, D. R., and Jimenez, J. L.: Field-deployable, high-resolution, time-of-flight aerosol mass spectrometer, Anal. Chem., 78, 8281–8289, doi:10.1021/ac061249n, 2006.

Gao, S., Ng, N. L., Keywood, M., Varutbangkul, V., Bahreini, R., Nenes, A., He, J. W., Yoo, K. Y., Beauchamp, J. L., Hodyss, R. P., Flagan, R. C., and Seinfeld, J. H.: Particle phase acidity and oligomer formation in secondary organic aerosol, Environ. Sci. Technol., 38, 6582–6589, doi:10.1021/es049125k, 2004a.

Gao, S., Keywood, M., Ng, N. L., Surratt, J., Varutbangkul, V., Bahreini, R., Flagan, R. C., and Seinfeld, J. H.: Low-molecular-weight and oligomeric components in secondary organic aerosol from the ozonolysis of cycloalkenes and alpha-pinene, J. Phys. Chem. A, 108, 10147–10164, doi:10.1021/jp047466e, 2004b.

Hallquist, M., Wenger, J. C., Baltensperger, U., Rudich, Y., Simpson, D., Claeys, M., Dommen, J., Donahue, N. M., George, C., Goldstein, A. H., Hamilton, J. F., Herrmann, H., Hoffmann, T., Iinuma, Y., Jang, M., Jenkin, M. E., Jimenez, J. L., Kiendler-Scharr, A., Maenhaut, W., McFiggans, G., Mentel, Th. F., Monod, A., Prévôt, A. S. H., Seinfeld, J. H., Surratt, J. D., Szmigielski, R., and Wildt, J.: The formation, properties and impact of secondary organic aerosol: current and emerging issues, Atmos. Chem. Phys., 9, 5155–5236, doi:10.5194/acp-9-5155-2009, 2009.

Hildebrandt, L., Donahue, N. M., and Pandis, S. N.: High formation of secondary organic aerosol from the photo-oxidation of toluene, Atmos. Chem. Phys., 9, 2973–2986, doi:10.5194/acp-9-2973-2009, 2009.

Kanakidou, M., Seinfeld, J. H., Pandis, S. N., Barnes, I., Dentener, F. J., Facchini, M. C., Van Dingenen, R., Ervens, B., Nenes, A., Nielsen, C. J., Swietlicki, E., Putaud, J. P., Balkanski, Y., Fuzzi, S., Horth, J., Moortgat, G. K., Winterhalter, R., Myhre, C. E. L., Tsigaridis, K., Vignati, E., Stephanou, E. G., and Wilson, J.: Organic aerosol and global climate modelling: a review, Atmos. Chem. Phys., 5, 1053–1123, doi:10.5194/acp-5-1053-2005, 2005.

Keywood, M. D., Varutbangkul, V., Bahreini, R., Flagan, R. C., and Seinfeld, J. H.: Secondary organic aerosol formation from the ozonolysis of cycloalkenes and related compounds, Environ. Sci. Technol., 38, 4157–4164, doi:10.1021/es035363o, 2004.

Kokkola, H., Yli-Pirilä, P., Vesterinen, M., Korhonen, H., Keskinen, H., Romakkaniemi, S., Hao, L., Kortelainen, A., Joutsensaari, J., Worsnop, D. R., Virtanen, A., and Lehtinen, K. E. J.: The role of low volatile organics on secondary organic aerosol formation, Atmos. Chem. Phys., 14, 1689–1700, doi:10.5194/acp-14-1689-2014, 2014.

Krechmer, J. E., Pagonis, D., Ziemann, P. J., and Jimenez, J. L.: Quantification of Gas-Wall Partitioning in Teflon Environmental Chambers Using Rapid Bursts of Low-Volatility Oxidized Species Generated in Situ, Environ. Sci. Technol., 50, 5757–5765, doi:10.1021/acs.est.6b00606, 2016.

Kroll, J. H. and Seinfeld, J. H.: Chemistry of secondary organic aerosol: Formation and evolution of low-volatility organics in the atmosphere, Atmos. Environ., 42, 3593–3624, doi:10.1016/j.atmosenv.2008.01.003, 2008.

La, Y. S., Camredon, M., Ziemann, P. J., Valorso, R., Matsunaga, A., Lannuque, V., Lee-Taylor, J., Hodzic, A., Madronich, S., and Aumont, B.: Impact of chamber wall loss of gaseous organic compounds on secondary organic aerosol formation: explicit modeling of SOA formation from alkane and alkene oxidation, Atmos. Chem. Phys., 16, 1417–1431, doi:10.5194/acp-16-1417-2016, 2016.

Loza, C. L., Chan, A. W. H., Galloway, M. M., Keutsch, F. N., Flagan, R. C., and Seinfeld, J. H.: Characterization of Vapor Wall Loss in Laboratory Chambers, Environ. Sci. Technol., 44, 5074–5078, doi:10.1021/es100727v, 2010.

Loza, C. L., Chhabra, P. S., Yee, L. D., Craven, J. S., Flagan, R. C., and Seinfeld, J. H.: Chemical aging of *m*-xylene secondary organic aerosol: laboratory chamber study, Atmos. Chem. Phys., 12, 151–167, doi:10.5194/acp-12-151-2012, 2012.

Matsunaga, A. and Ziemann, P. J.: Gas-Wall Partitioning of Organic Compounds in a Teflon Film Chamber and Potential Effects on Reaction Product and Aerosol Yield Measurements, Aerosol Sci. Tech., 44, 881–892, doi:10.1080/02786826.2010.501044, 2010.

McMurry, P. H. and Grosjean, D.: Gas and Aerosol Wall Losses in Teflon Film Smog Chambers, Environ. Sci. Technol., 19, 1176–1182, doi:10.1021/es00142a006, 1985.

McMurry, P. H. and Rader, D. J.: Aerosol Wall Losses in Electrically Charged Chambers, Aerosol Sci. Tech., 4, 249–268, doi:10.1080/02786828508959054, 1985.

McVay, R. C., Cappa, C. D., and Seinfeld, J. H.: Vapor-Wall Deposition in Chambers: Theoretical Considerations, Environ. Sci. Technol., 48, 10251–10258, doi:10.1021/es502170j, 2014.

McVay, R. C., Zhang, X., Aumont, B., Valorso, R., Camredon, M., La, Y. S., Wennberg, P. O., and Seinfeld, J. H.: SOA formation from the photooxidation of α-pinene: systematic exploration of the simulation of chamber data, Atmos. Chem. Phys., 16, 2785–2802, doi:10.5194/acp-16-2785-2016, 2016.

Nah, T., McVay, R. C., Zhang, X., Boyd, C. M., Seinfeld, J. H., and Ng, N. L.: Influence of seed aerosol surface area and oxidation rate on vapor wall deposition and SOA mass yields: a case study with α-pinene ozonolysis, Atmos. Chem. Phys., 16, 9361–9379, doi:10.5194/acp-16-9361-2016, 2016.

Ng, N. L., Kroll, J. H., Keywood, M. D., Bahreini, R., Varutbangkul, V., Flagan, R. C., Seinfeld, J. H., Lee, A., and Goldstein, A. H.: Contribution of first- versus second-generation products to secondary organic aerosols formed in the oxidation of biogenic hydrocarbons, Environ. Sci. Technol., 40, 2283–2297, doi:10.1021/es052269u, 2006.

Odum, J. R., Hoffmann, T., Bowman, F., Collins, D., Flagan, R. C., and Seinfeld, J. H.: Gas/Particle Partitioning and Secondary Organic Aerosol Yields, Environ. Sci. Technol., 30, 2580–2585, doi:10.1021/es950943+, 1996.

Odum, J. R., Jungkamp, T. P. W., Griffin, R. J., Flagan, R. C., and Seinfeld, J. H.: The atmospheric aerosol-forming potential of whole gasoline vapor, Science, 276, 96–99, doi:10.1126/science.276.5309.96, 1997a.

Odum, J. R., Jungkamp, T. P. W., Griffin, R. J., Forstner, H. J. L., Flagan, R. C., and Seinfeld, J. H.: Aromatics, reformulated gasoline, and atmospheric organic aerosol formation, Environ. Sci. Technol., 31, 1890–1897, doi:10.1021/es960535l, 1997b.

Pathak, R. K., Stanier, C. O., Donahue, N. M., and Pandis, S. N.: Ozonolysis of alpha-pinene at atmospherically relevant concentrations: Temperature dependence of aerosol mass fractions (yields), J. Geophys. Res.-Atmos., 112, D03201, doi:10.1029/2006jd007436, 2007.

Pierce, J. R., Engelhart, G. J., Hildebrandt, L., Weitkamp, E. A., Pathak, R. K., Donahue, N. M., Robinson, A. L., Adams, P. J., and Pandis, S. N.: Constraining particle evolution from wall losses, coagulation, and condensation-evaporation in smog-chamber experiments: Optimal estimation based on size distribution measurements, Aerosol Sci. Tech., 42, 1001–1015, doi:10.1080/02786820802389251, 2008.

Riipinen, I., Pierce, J. R., Yli-Juuti, T., Nieminen, T., Häkkinen, S., Ehn, M., Junninen, H., Lehtipalo, K., Petäjä, T., Slowik, J., Chang, R., Shantz, N. C., Abbatt, J., Leaitch, W. R., Kerminen, V.-M., Worsnop, D. R., Pandis, S. N., Donahue, N. M., and Kulmala, M.: Organic condensation: a vital link connecting aerosol formation to cloud condensation nuclei (CCN) concentrations, Atmos. Chem. Phys., 11, 3865–3878, doi:10.5194/acp-11-3865-2011, 2011.

Saleh, R., Donahue, N. M., and Robinson, A. L.: Time Scales for Gas-Particle Partitioning Equilibration of Secondary Organic Aerosol Formed from Alpha-Pinene Ozonolysis, Environ. Sci. Technol., 47, 5588–5594, doi:10.1021/es400078d, 2013.

Seinfeld, J. H. and Pandis, S. N.: Atmospheric chemistry and physics: from air pollution to climate change, Third edition, John Wiley & Sons, Inc., Hoboken, New Jersey, USA, 1120 pp., 2016.

Shiraiwa, M. and Seinfeld, J. H.: Equilibration timescale of atmospheric secondary organic aerosol partitioning, Geophys. Res. Lett., 39, L24801, doi:10.1029/2012gl054008, 2012.

Tsigaridis, K., Daskalakis, N., Kanakidou, M., Adams, P. J., Artaxo, P., Bahadur, R., Balkanski, Y., Bauer, S. E., Bellouin, N., Benedetti, A., Bergman, T., Berntsen, T. K., Beukes, J. P., Bian, H., Carslaw, K. S., Chin, M., Curci, G., Diehl, T., Easter, R. C., Ghan, S. J., Gong, S. L., Hodzic, A., Hoyle, C. R., Iversen, T., Jathar, S., Jimenez, J. L., Kaiser, J. W., Kirkevåg, A., Koch, D., Kokkola, H., Lee, Y. H., Lin, G., Liu, X., Luo, G., Ma, X., Mann, G. W., Mihalopoulos, N., Morcrette, J.-J., Müller, J.-F., Myhre, G., Myriokefalitakis, S., Ng, N. L., O'Donnell, D., Penner, J. E., Pozzoli, L., Pringle, K. J., Russell, L. M., Schulz, M., Sciare, J., Seland, Ø., Shindell, D. T., Sillman, S., Skeie, R. B., Spracklen, D., Stavrakou, T., Steenrod, S. D., Takemura, T., Tiitta, P., Tilmes, S., Tost, H., van Noije, T., van Zyl, P. G., von Salzen, K., Yu, F., Wang, Z., Wang, Z., Zaveri, R. A., Zhang, H., Zhang, K., Zhang, Q., and Zhang, X.: The AeroCom evaluation and intercomparison of organic aerosol in global models, Atmos. Chem. Phys., 14, 10845–10895, doi:10.5194/acp-14-10845-2014, 2014.

Weitkamp, E. A., Sage, A. M., Pierce, J. R., Donahue, N. M., and Robinson, A. L.: Organic aerosol formation from photochemical oxidation of diesel exhaust in a smog chamber, Environ. Sci. Technol., 41, 6969–6975, doi:10.1021/es070193r, 2007.

Ye, P., Ding, X., Hakala, J., Hofbauer, V., Robinson, E. S., and Donahue, N. M.: Vapor wall loss of semi-volatile organic compounds in a Teflon chamber, Aerosol Sci. Tech., 50, 822–834, doi:10.1080/02786826.2016.1195905, 2016.

Yeh, G. K. and Ziemann, P. J.: Alkyl Nitrate Formation from the Reactions of C-8-C-14 n-Alkanes with OH Radicals in the Presence of NO_x: Measured Yields with Essential Corrections for Gas-Wall Partitioning, J. Phys. Chem. A, 118, 8147–8157, doi:10.1021/jp500631v, 2014.

Yeh, G. K. and Ziemann, P. J.: Gas-Wall Partitioning of Oxygenated Organic Compounds: Measurements, Structure-Activity Relationships, and Correlation with Gas Chromatographic Retention Factor, Aerosol Sci. Tech., 49, 726–737, doi:10.1080/02786826.2015.1068427, 2015.

Zhang, X., Pandis, S. N., and Seinfeld, J. H.: Diffusion-Limited Versus Quasi-Equilibrium Aerosol Growth, Aerosol Sci. Tech., 46, 874–885, doi:10.1080/02786826.2012.679344, 2012.

Zhang, X., Cappa, C. D., Jathar, S. H., McVay, R. C., Ensberg, J. J., Kleeman, M. J., and Seinfeld, J. H.: Influence of vapor wall loss in laboratory chambers on yields of secondary organic aerosol, P. Natl. Acad. Sci. USA, 111, 5802–5807, doi:10.1073/pnas.1404727111, 2014.

Zhang, X., Schwantes, R. H., McVay, R. C., Lignell, H., Coggon, M. M., Flagan, R. C., and Seinfeld, J. H.: Vapor wall deposition in Teflon chambers, Atmos. Chem. Phys., 15, 4197–4214, doi:10.5194/acp-15-4197-2015, 2015.